01 Sep 2016

Room-Temperature Electrochemical Reduction of Epitaxial Bi_2O_3 Films to Epitaxial Bi Films

Zhen He

Jakub Adam Koza

Ying-Chau Liu

Qingzhi Chen

et. al. For a complete list of authors, see https://scholarsmine.mst.edu/chem_facwork/2640

Recommended Citation

Z. He et al., "Room-Temperature Electrochemical Reduction of Epitaxial Bi_2O_3 Films to Epitaxial Bi Films," *RSC Advances*, vol. 6, no. 99, pp. 96832-96836, Royal Society of Chemistry, Sep 2016.
The definitive version is available at https://doi.org/10.1039/c6ra18098a

RSC Advances

COMMUNICATION

View Article Online
View Journal | View Issue

Cite this: *RSC Adv.*, 2016, **6**, 96832

Room-temperature electrochemical reduction of epitaxial Bi_2O_3 films to epitaxial Bi films†

Zhen He,*[ab] Jakub A. Koza,[b] Ying-Chau Liu,[b] Qingzhi Chen[b] and Jay A. Switzer[b]

Received 15th July 2016
Accepted 29th September 2016

DOI: 10.1039/c6ra18098a

www.rsc.org/advances

This work reports a new facile approach to fabricate high-quality epitaxial Bi thin films by direct electrochemical reduction of epitaxial δ-Bi_2O_3 thin films on Au single crystals in aqueous solution at room-temperature. The as-produced Bi thin films (without any post-annealing process) exhibit large grain sizes, continuous microstructures, and enhanced magnetotransport properties.

Semimetal bismuth (Bi) has been intensively studied for quantum transport and finite size effects because it exhibits unusual electronic and magnetotransport properties due to its highly anisotropic Fermi surface, low carrier densities, small carrier effective masses, and long carrier mean free paths.[1–5] A large magnetoresistance (MR) effect has been found in bulk single crystals of Bi.[6,7] As a result, Bi has been regarded as one of the most promising materials in technological applications including magnetic field sensing and spintronics.[8] For realization of these technological applications, high-quality Bi thin films with properties (*e.g.*, large MR) similar to bulk single-crystal Bi are required.[5,9]

The transport properties of crystalline Bi thin films greatly depend on the microstructures and are varied with their crystallographic orientations due to the highly anisotropic Fermi surface.[4,10] Generally, smooth, continuous, and single-crystalline Bi thin films with large grains are found to have optimized transport properties such as large MR.[3–5,11–13] However, the fabrication of high-quality, and morphology-, structure-, and orientation-controlled thin films of Bi is still challenging.[4,14] Traditional vapour deposition techniques such as thermal evaporation and sputtering produce polycrystalline Bi films consisting of small-size grains.[15,16] These Bi films usually show small mean free paths with a MR that is several orders of magnitude smaller compared to that of the bulk single-crystal Bi.[3,5] High-quality Bi thin films with well-controlled preferred orientations have been produced by molecular beam epitaxy (MBE) and pulsed laser deposition (PLD) on various substrates, including BaF_2, Si, and glass.[2,10,13,17] However, these ultrahigh-vacuum and specialized growth techniques are costly and time-consuming, and therefore are not suitable for large-scale fabrication of high-quality Bi thin films for application purposes. Searson and co-workers demonstrated that single-crystal Bi thin films with very large MR could be grown onto an Au/Si(100) substrate from an aqueous solution of $Bi(NO_3)_3 \cdot 5H_2O$ by electrodeposition and suitable annealing.[3,5,18] Bi thin films made by this method exhibit MR up to 300% at 300 K and 400 000% at 5 K.[18] Highly textured or epitaxial Bi films have also been electrodeposited onto various substrates, such as Au and GaAs single crystals of different orientations.[19–21] The deposition parameters, such as applied potential/current density, Bi(III) concentration in the deposition solution, and film thickness, have remarkably strong influences on the microstructures and morphologies of the as-deposited Bi films.[4] The orientations of the Bi films after annealing are dependent on the initial microstructures of the as-deposited films and the substrates.[4,12] Compared to MBE or PLD, electrodeposition has a much lower cost and therefore is more applicable for large-scale production of high-quality Bi films. However, the as-deposited Bi films are in fact polycrystalline. The post-annealing step (at 268 °C for 6 hours in Ar) is critical for the transformation of the polycrystalline Bi films to large-grained and single-crystalline Bi films with the trigonal axis oriented perpendicular to the film plane.[5] Despite the advantages of electrodeposition, the post-annealing process is undesired for the application of Bi thin films in areas such as spintronics.[4] More recently, the epitaxial growth of single-crystalline Bi thin films by direct electrodeposition has been reported.[22,23] However, the microstructures of these Bi films are

[a]*College of Chemistry and Chemical Engineering, Central South University, Changsha, Hunan 410083, P. R. China. E-mail: zhenhe@csu.edu.cn*

[b]*Department of Chemistry and Graduate Center for Materials Research, Missouri University of Science and Technology, Rolla, Missouri 65401-1170, USA*

† Electronic supplementary information (ESI) available: Experimental details, calculations of the volume change from Bi_2O_3 thin films to Bi thin films, XPS and EDS investigations, determination of the epitaxial relationships between the Bi_2O_3 film and Au(111), and between the Bi film and Au(111). See DOI: 10.1039/c6ra18098a

either needle-like, triangular, or pyramidal islands, which result in poor transport properties.[4] Therefore, the production of as-deposited Bi thin films with well-controlled orientations, desired microstructures, and optimized transport properties remains a significant technological challenge.

Here, we present a new facile approach to produce epitaxial Bi thin films with a continuous microstructure by direct electrochemical reduction of predeposited epitaxial δ-Bi_2O_3 thin films on Au single crystals in aqueous solution at room-temperature. The as-produced Bi thin films are epitaxial without any post processing treatment. The electrochemical reduction of metal oxides to the corresponding metals has been studied for decades as an alternative to pyrometallurgical processes for the metallurgy industry. Elemental metals and semiconductors, including Ti, Fe, Cu, Zr, and Si, have been produced using this concept.[24–32] We have demonstrated in previous work that epitaxial Fe_3O_4 thin films on Au single crystals could be electrochemically reduced to epitaxial Fe thin films in aqueous solution at room-temperature.[33]

Our motivation to study the epitaxial transformation of δ-Bi_2O_3 thin films to Bi thin films by direct electrochemical reduction is multifold. First, this is a new and facile method to fabricate epitaxial Bi thin films without post-annealing and could possibly produce Bi films with unique microstructures. Second, this could help us in understanding the mechanism of solid oxide electrochemical reduction. For example, the mechanism of the Fe_3O_4 reduction to Fe could be either direct solid-to-solid transformation or dissolution/re-deposition because soluble intermediates such as $Fe(OH)_3^-$ could exist during the reduction process.[33] However, there is no intermediate oxidation state for bismuth between Bi^{3+} (in Bi_2O_3) and Bi^0 (in elemental Bi), and Bi_2O_3 has the highest known oxide ion mobility among metal oxides. Therefore, the reduction of Bi_2O_3 to Bi is more likely through the direct solid-to-solid transformation. Third, this is interesting due to the drastic structure and volume changes during the Bi_2O_3-to-Bi conversion. δ-Bi_2O_3 has a cubic structure ($Fm3m$, $a = 0.5525$ nm), whereas Bi is rhombohedral ($R\bar{3}m$, $a = 0.474$ nm, $\alpha = 57°14'$). Furthermore, this work could contribute to the understanding of resistance switching in metal oxides, in which the formation of metallic filaments is involved.[34,35]

The potential window of the electrochemical reduction of Bi_2O_3 to Bi was studied in 2 M NaOH at room-temperature by linear sweep voltammetry (LSV) at a scan rate of 10 mV s^{-1} from the open circuit potential (OCP) to about −1.4 V *vs.* Ag/AgCl as shown in Fig. 1. The LSV on a bare Au electrode (blue curve) shows no significant cathodic current in this potential window, whereas the LSV on a predeposited δ-Bi_2O_3 film (red curve) on the Au electrode shows a major cathodic peak at about −1.06 V *vs.* Ag/AgCl. This cathodic peak is due to the reduction of the predeposited δ-Bi_2O_3 film. Besides, there is a minor cathodic peak at about −0.64 V *vs.* Ag/AgCl. This peak could probably arise from the reduction of a small amount of Bi_2O_5 impurity in the δ-Bi_2O_3 film, since the mechanism of δ-Bi_2O_3 electrodeposition involves the formation and decomposition of Bi_2O_5 as an intermediate.[36] The insets in Fig. 1 are photographs of the predeposited δ-Bi_2O_3 film on the Au electrode before and after

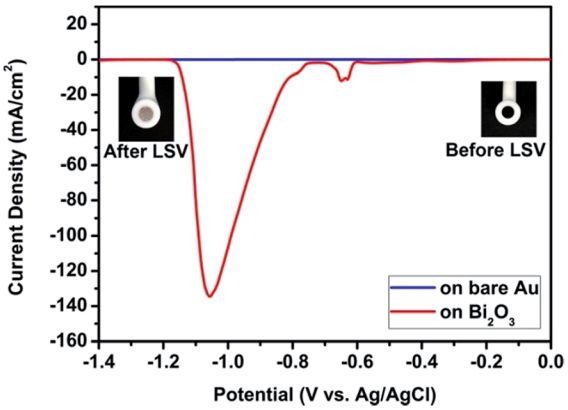

Fig. 1 Linear sweep voltammograms on a bare Au electrode and on a δ-Bi_2O_3 film predeposited on the Au electrode. The voltammograms were run at a scan rate of 10 mV s^{-1} in an unstirred 2 M NaOH solution. The insets are photographs of the Au electrode with a predeposited δ-Bi_2O_3 film before and after the LSV test.

the LSV scan. Before the LSV scan, the predeposited Bi_2O_3 film is dark brownish-black. After the LSV scan, the Bi_2O_3 film appears to be reduced to a silver-colored metallic Bi film. The surface layer of the Bi film after reduction seems rough and even exfoliated at some parts. This layer consists of metallic Bi and unreduced Bi_2O_3, and could be easily removed by flushing with distilled water or by using an adhesive tape. Considering a large volume expansion (about 51.3%, see calculations in ESI†) and difficulties of oxide ion transport in solids during the solid transformation of δ-Bi_2O_3 to metallic Bi, it is not a surprise that some of the Bi_2O_3 film could not stand the drastic structure change and exfoliate. After the thin rough surface layer is removed, the remaining Bi layer adheres well on the Au substrate and has a smooth and shiny metallic appearance.

The crystal structures of the predeposited δ-Bi_2O_3 film and the Bi film after reduction were characterized by XRD. The Bi_2O_3 film was electrochemically deposited on a Au(111) single crystal.[37] This film was then reduced in 2 M NaOH at room-temperature by applying a constant potential of −0.8 V *vs.* Ag/AgCl (see experimental details in ESI†), which is close to the onset point of the major reduction peak of Bi_2O_3 in the LSV. This potential was intentionally chosen to ensure a proper reduction rate in order to obtain a more uniform Bi layer. Too rapid film reduction could result in severe exfoliation of the film due to the large volume change and relatively slow oxide ion mobility in solids. The XRD θ–2θ scans of a predeposited Bi_2O_3 film (black line) and the Bi film after reduction (red line) on a Au(111) single crystal are shown in Fig. 2a. As shown in our previous work, the Bi_2O_3 film electrodeposited on Au(111) grows with a [111] out-of-plane orientation.[37] After reduction, the θ–2θ diffraction pattern of the produced metallic layer matches with the rhombohedral Bi with a [012] out-of-plane orientation (please note that the Bi is indexed in the hexagonal system.[18,19] See Fig. S1 in ESI†). The comparison between the X-ray photoelectron spectra (XPS) of the predeposited Bi_2O_3 film and the Bi film after reduction also shows that the oxidation state of Bi changes from Bi^{3+} in the Bi_2O_3 film to Bi^0 in the Bi film after

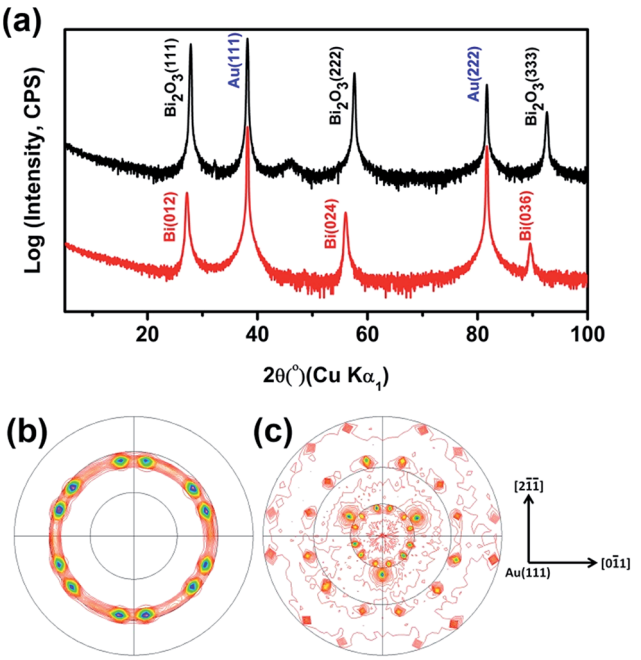

Fig. 2 X-ray diffraction characterization of an electrodeposited δ-Bi_2O_3 film and the corresponding Bi film electrochemically reduced from the precursor δ-Bi_2O_3 film. (a) θ–2θ scans of the δ-Bi_2O_3 film (black curve) and the Bi film (red curve) on Au(111). (b) A (200) pole figure of the δ-Bi_2O_3 film on Au(111). (c) A (116) pole figure of the Bi film on Au(111). The in-plane orientations of the Au(111) substrate are shown as the arrows with directions.

reduction (see Fig. S2 in ESI†). The energy dispersive spectroscopy investigation further reveals that the resultant shiny metallic film reduced from the predeposited Bi_2O_3 film is nearly 100% Bi (see Table S1 in ESI†). The XRD, XPS, and EDS results agree well, suggesting the formation of metallic, trigonal Bi film from the reduction of the predeposited cubic Bi_2O_3 film.

Texture analysis was used to probe the in-plane orientations of the predeposited Bi_2O_3 film and the Bi film after reduction. The (200) pole figure of a predeposited Bi_2O_3 film on a Au(111) single crystal and the (116) pole figure of the Bi film after electrochemical reduction are shown in Fig. 2b and c, respectively. The pole figures show that the cubic Bi_2O_3 is transformed to trigonal Bi. Both pole figures show spot patterns instead of ring patterns, indicating that both films are not only out-of-plane oriented but also in-plane oriented. That is, these films are epitaxial. The (311) pole figure of the Au(111) substrate was also obtained (Fig. S3h†) and the in-plane orientations of the Au(111) substrate are shown as the arrows with directions in Fig. 2. By comparing the measured pole figures with the corresponding stereographic projections (Fig. S3 and S4†), the epitaxial relationships between the δ-Bi_2O_3 film and the Au(111) substrate, as well as the epitaxial relationships between the Bi film and the Au(111) substrate, are determined. The (200) pole figure of a single domain Bi_2O_3(111) film on Au(111) should show three-fold symmetry (Fig. S3a†). That is, three equally spaced (azimuthally spaced with $\Delta\varphi = 120°$) peaks should appear at a tilt angle, χ, of 54.7°, which is the interplanar angle between the {111} and {200} planes of Bi_2O_3. In the measured Bi_2O_3 pole figure, there are twelve peaks at the tilt angle of 54.7° (Fig. 2b), indicating there are four domains of Bi_2O_3 with the same out-of-plane orientation (*i.e.*, [111]) but different in-plane orientations on Au(111). These four domains of Bi_2O_3 could be explained as follows. The single domain of Bi_2O_3 rotates about ±10.9° relative to the Au substrate, suggesting that the Bi_2O_3 film might consist of misoriented microdomains, with defects such as stacking faults at the domain boundaries.[37] Besides, each rotated domain of Bi_2O_3 has an antiparalleled domain, resulting in a total of four domains. Therefore, the epitaxial relationships between the four domains of Bi_2O_3(111) and Au(111) are, $Bi_2O_3(111)[2\bar{1}\bar{1}]||Au(111)[3\bar{2}\bar{1}]$, $Bi_2O_3(111)[\bar{2}11]||Au(111)[3\bar{2}\bar{1}]$, $Bi_2O_3(111)[2\bar{1}\bar{1}]||Au(111)[3\bar{1}\bar{2}]$, and $Bi_2O_3(111)[\bar{2}11]||Au(111)[3\bar{1}\bar{2}]$ (see details in Fig. S3†).

For the (116) pole figure of the Bi thin film, single domain of Bi(012) should have two diffraction peaks at each of the tilt angles of about 27.0°, 65.3°, and 86.8° (Fig. S4a†). However, the measured (116) pole figure of Bi(012) film on Au(111) has twelve diffraction peaks at each of these tilt angles. This indicates that there are six domains of Bi(012) on Au(111), which are separated azimuthally by 60.0°. The three extra diffraction peaks at the tilt angle of about 35.3° in the measured Bi(116) pole figure arise from the Au(111) substrate (see details in Fig. S4†). Therefore, the epitaxial relationships of the Bi(012) film on Au(111) are, $Bi(012)[01\bar{1}]||Au(111)[\bar{1}\bar{1}2]$, $Bi(012)[01\bar{1}]||Au(111)[11\bar{2}]$, $Bi(012)[01\bar{1}]||Au(111)[1\bar{2}1]$, $Bi(012)[01\bar{1}]||Au(111)[\bar{1}2\bar{1}]$, $Bi(012)[01\bar{1}]||Au(111)[2\bar{1}\bar{1}]$, $Bi(012)[01\bar{1}]||Au(111)[\bar{2}11]$ (see details in Fig. S4†). Bi films with the trigonal axis oriented perpendicular to the film plane (*i.e.*, Bi(001) thin films) show the highest MR.[5,11] Since the deposition parameters and annealing temperatures strongly affect the orientations of the Bi thin films, it will be interesting to try different experimental parameters (*e.g.*, elevated temperatures, other types of single crystalline substrates) used in electrochemical reduction of Bi_2O_3 to see if (001) epitaxial Bi films can be produced in further research.

The plan-view SEM images of an epitaxial Bi thin film produced by electrochemical reduction of a predeposited Bi_2O_3 thin film on a Au(111) single crystal are shown in Fig. 3. It is well documented that the microstructure of the electrodeposited Bi thin film is dependent on many parameters such as deposition temperature, potential, and film thickness.[4] Bi thin films directly electrodeposited on Au substrates are usually composed of discontinuous pyramidal or needle-like grains loosely stacking with each other,[4] whereas Bi films directly electrodeposited on GaAs(111) substrates shows nanometer-scale triangular grains aligned on the surface.[23] The morphologies of these directly electrodeposited Bi thin films do not match with the microstructural features of Bi films (*i.e.*, continuous films with a large grain size and less grain boundaries) showing good transport properties. However, in our case, the produced epitaxial Bi thin film after reduction on Au(111) presents well-aligned elongated polyhedrons closely cross-linking with each other. The length of the elongated polyhedrons could be up to several micrometers. The film looks more continuous and has a larger apparent grain size than the direct electrodeposited Bi films.[4,23] These microstructural features might contribute to better transport properties of the Bi thin film.

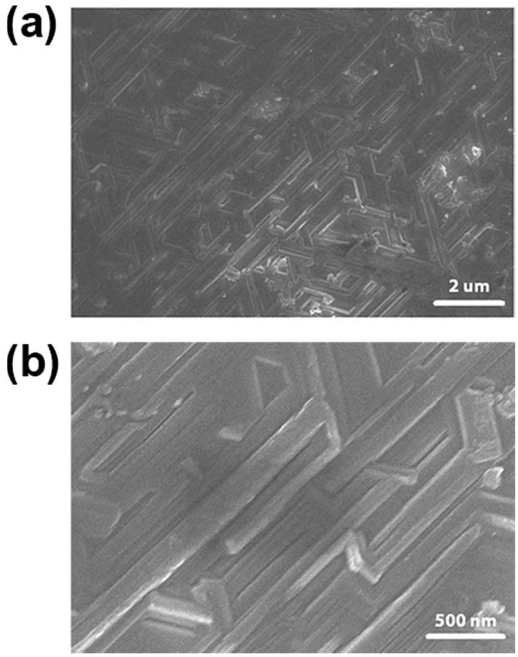

Fig. 3 SEM images at magnifications of (a) 10k and (b) 45k of a Bi film produced by electrochemically reducing a predeposited δ-Bi_2O_3 film on Au(111).

To analyze the magnetotransport property of the Bi thin film, MR measurement was performed on the Bi thin film on Au(111). Fig. 4 shows the MR ratio for the Bi film in response to a magnetic field in perpendicular (*P*) geometry at 77 K. That is, the magnetic field was along the out-of-plane orientation of the film and perpendicular to the direction of current flow, as shown by the inset cartoon in Fig. 4. In the range of the magnetic field used in our measurement, the largest MR ratio is about 3.2% at 50 kOe and the MR shows no evidence of saturation in the range. It has been reported that the MR of electrodeposited Bi thin films is strongly related to the crystallinity, orientation, grain size, annealing temperature, temperature of measurements, and the direction of the applied magnetic field.[4,18] Generally, single-crystalline (001) Bi films annealed at a temperature (*e.g.*, 268 °C) close to the melting temperature of Bi measured in a *P* geometry at very low temperatures (*e.g.*, 5 K) give the highest MR values. Although our measured MR value of the Bi film is much lower than the highest reported MR values for the electrodeposited Bi films with post annealing, it is comparable with the reported MR value of an as-deposited (012) Bi thin film measured in *P* geometry at 10 K.[4] Considering our MR measurement was performed at a much higher temperature (*i.e.*, 77 K), our Bi film produced by the direct electrochemical reduction of a δ-Bi_2O_3 film should have better magnetotransport properties compared to the direct electrodeposited Bi films under the same conditions of measurements. This could be attributed to the more continuous microstructures and larger grain sizes of our Bi films.

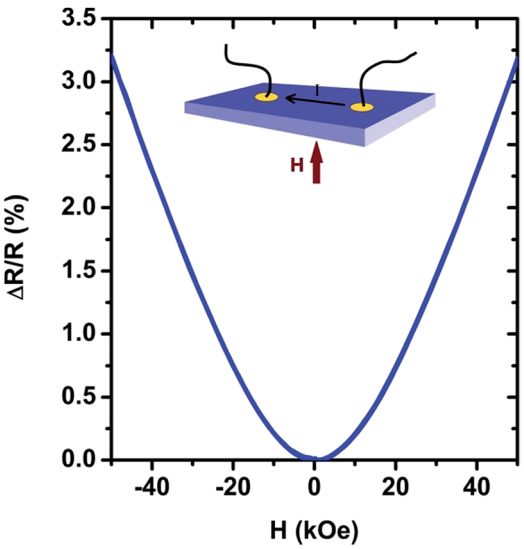

Fig. 4 Magnetoresistance of a Bi film produced by electrochemically reducing a predeposited δ-Bi_2O_3 film on Au(111). The measurement was performed at 77 K with the magnetic field applied along the out-of-plane orientation of the film and perpendicular to current as shown by the inset cartoon.

Conclusions

High-quality epitaxial Bi thin films were produced by direct electrochemical reduction of predeposited δ-Bi_2O_3 films on single crystals of Au in aqueous solution at room-temperature. The as-grown Bi films are fully crystalline and epitaxial without any post annealing process. Compared to directly electrodeposited Bi films, our Bi films show a larger apparent grain size and more continuous microstructure. The produced Bi film shows a 3.2% magnetoresistance in a magnetic field of 50 kOe at 77 K, which is comparable with that of a directly electrodeposited Bi film measured at 10 K. The fabrication of metallic thin films by direct electrochemical reduction of the corresponding metal oxide thin films opens new possibilities to produce metal and alloy thin films with different microstructures and improved magnetotransport and electronic properties. Furthermore, since the deposition parameters and annealing temperatures strongly affect the microstructures and orientations of the Bi thin films, it would be interesting to see how the parameters used in electrochemical reduction of Bi_2O_3 affect the morphologies, crystalline orientations, and magnetotransport properties of the produced Bi thin films.

Acknowledgements

The work at Central South University was supported by the Natural Science Foundation of Hunan Province, China (Grant No. 2015JJ3144), National Natural Science Foundation of China (Grant No. 21303270), and Scientific Research Foundation for the Returned Overseas Chinese Scholars, Ministry of Education of P. R. China (Grant No. 2013[1792]). The work at Missouri University of Science and Technology was supported by the U. S. Department of Energy, Office of Basic Energy Science (Grant No. DE-FG02-08ER46518).

References

1 R. Hartman, *Phys. Rev.*, 1969, **181**, 1070–1086.
2 M. Lu, R. J. Zieve, A. van Hulst, H. M. Jaeger, T. F. Rosenbaum and S. Radelaar, *Phys. Rev. B: Condens. Matter Mater. Phys.*, 1996, **53**, 1609–1615.
3 F. Y. Yang, K. Liu, C. L. Chien and P. C. Searson, *Phys. Rev. Lett.*, 1999, **82**, 3328–3331.
4 B. O'Brien, M. Plaza, L. Y. Zhu, L. Perez, C. L. Chien and P. C. Searson, *J. Phys. Chem. C*, 2008, **112**, 12018–12023.
5 F. Y. Yang, K. Liu, K. Hong, D. H. Reich, P. C. Searson and C. L. Chien, *Science*, 1999, **284**, 1335–1337.
6 J. H. Mangez, J. P. Issi and J. Heremans, *Phys. Rev. B: Solid State*, 1976, **14**, 4381–4385.
7 P. B. Alers and R. T. Webber, *Phys. Rev.*, 1953, **91**, 1060–1065.
8 G. A. Prinz, *Science*, 1998, **282**, 1660–1663.
9 N. Marcano, S. Sangiao, J. M. De Teresa, L. Morellon, M. R. Ibarra, M. Plaza and L. Perez, *J. Magn. Magn. Mater.*, 2010, **322**, 1460–1463.
10 K. S. Wu and M.-Y. Chern, *Thin Solid Films*, 2008, **516**, 3808–3812.
11 S. Cho, Y. Kim, A. J. Freeman, G. K. L. Wong, J. B. Ketterson, L. J. Olafsen, I. Vurgaftman, J. R. Meyer and C. A. Hoffman, *Appl. Phys. Lett.*, 2001, **79**, 3651–3653.
12 J.-H. Hsu, Y.-S. Sun, H.-X. Wang, P. C. Kuo, T.-H. Hsieh and C.-T. Liang, *J. Magn. Magn. Mater.*, 2004, **272–276**, 1769–1771.
13 D. L. Partin, J. Heremans, D. T. Morelli, C. M. Thrush, C. H. Olk and T. A. Perry, *Phys. Rev. B: Condens. Matter Mater. Phys.*, 1988, **38**, 3818–3824.
14 X. Du and A. F. Hebard, *Appl. Phys. Lett.*, 2003, **82**, 2293–2295.
15 D. E. Beutler and N. Giordano, *Phys. Rev. B: Condens. Matter Mater. Phys.*, 1988, **38**, 8–19.
16 T. Missana and C. N. Afonso, *Appl. Phys. A*, 1996, **62**, 513–518.
17 J. C. G. de Sande, T. Missana and C. N. Afonso, *J. Appl. Phys.*, 1996, **80**, 7023–7027.
18 C. L. Chien, F. Y. Yang, K. Liu, D. H. Reich and P. C. Searson, *J. Appl. Phys.*, 2000, **87**, 4659–4664.
19 P. M. Vereecken, L. Sun, P. C. Searson, M. Tanase, D. H. Reich and C. L. Chien, *J. Appl. Phys.*, 2000, **88**, 6529–6535.
20 P. M. Vereecken, K. Rodbell, C. Ji and P. C. Searson, *Appl. Phys. Lett.*, 2005, **86**, 121916.
21 F. Y. Yang, G. J. Strijkers, K. Hong, D. H. Reich, P. C. Searson and C. L. Chien, *J. Appl. Phys.*, 2001, **89**, 7206–7208.
22 C. A. Jeffrey, S. H. Zheng, E. Bohannan, D. A. Harrington and S. Morin, *Surf. Sci.*, 2005, **600**, 95–105.
23 Z. L. Bao and K. L. Kavanagh, *Appl. Phys. Lett.*, 2006, **88**, 022102.
24 G. Z. Chen, D. J. Fray and T. W. Farthing, *Nature*, 2000, **407**, 361–364.
25 A. Cox and D. J. Fray, *J. Appl. Electrochem.*, 2008, **38**, 1401–1407.
26 A. Allanore, H. Lavelaine, G. Valentin, J. P. Birat and F. Lapicque, *J. Electrochem. Soc.*, 2008, **155**, E125–E129.
27 A. Allanore, H. Lavelaine, G. Valentin, J. P. Birat, P. Delcroix and F. Lapicque, *Electrochim. Acta*, 2010, **55**, 4007–4013.
28 T. Nohira, K. Yasuda and Y. Ito, *Nat. Mater.*, 2003, **2**, 397–401.
29 X. Jin, P. Gao, D. Wang, X. Hu and G. Z. Chen, *Angew. Chem., Int. Ed.*, 2004, **43**, 733–736.
30 W. Xiao, X. Jin, Y. Deng, D. Wang and G. Z. Chen, *J. Electroanal. Chem.*, 2010, **639**, 130–140.
31 J. Peng, K. Jiang, W. Xiao, D. Wang, X. Jin and G. Z. Chen, *Chem. Mater.*, 2008, **20**, 7274–7280.
32 W.-K. Han, J.-W. Choi, G.-H. Hwang, S.-J. Hong, J.-S. Lee and S.-G. Kang, *Appl. Surf. Sci.*, 2006, **252**, 2832–2838.
33 Z. He, R. V. Gudavarthy, J. A. Koza and J. A. Switzer, *J. Am. Chem. Soc.*, 2011, **133**, 12358–12361.
34 J. A. Koza, E. W. Bohannan and J. A. Switzer, *ACS Nano*, 2013, **7**, 9940–9946.
35 J. A. Koza, I. P. Schroen, M. M. Willmering and J. A. Switzer, *Chem. Mater.*, 2014, **26**, 4425–4432.
36 E. W. Bohannan, C. C. Jaynes, M. G. Shumsky, J. K. Barton and J. A. Switzer, *Solid State Ionics*, 2000, **131**, 97–107.
37 J. A. Switzer, M. G. Shumsky and E. W. Bohannan, *Science*, 1999, **284**, 293–296.

